

# The Effect of Basalt Material Composition and Rice Husk Ash on The Characterization of Paving Block

M Amin<sup>1\*</sup>, Sudiby<sup>1</sup>, M Jannah<sup>2</sup> and P Karo-Karo<sup>2</sup>

<sup>1</sup>Mineral Technology Research Institute, LIPI, South Lampung, Lampung, 35361

<sup>2</sup>Department of Physics, FMIPA, University of Lampung, Bandar Lampung, 35141

\*Email: [muha047@lipi.go.id](mailto:muha047@lipi.go.id), [sudibyochemeng@gmail.com](mailto:sudibyochemeng@gmail.com)

## Article Information:

Received:  
21 March 2021

Received in revised form:  
7 May 2021

Accepted:  
25 May 2021

Volume 3, Issue 1, June 2021  
pp. 13 – 18

<http://doi.org/10.23960/jesr.v3i1.63>

## Abstract

*Paving block (concrete brick) is a composition of building materials made from a mixture of Portland cement or other hydraulic adhesive. The production process includes molding, soaking, physical testing such as compressive strength, density, porosity, and absorption, as well as characterization, namely X-Ray Diffraction (XRD) and X-Ray Fluorescence (XRF). Paving block was produced both without additives and with the inclusion of basalt stone and rice husk ash at proportions of 5%, 10%, 15%, 20%, and 25%, and tested after curing periods of 7, 14, and 28 days. The materials used were cement, sand, basalt stone, rice husk ash, and water. Paving block without the additives had the highest compressive strength at the test age of 28 days of 9.9 MPa and absorption of 15.06%. The addition of basalt stone and rice husk ash recorded the highest compressive strength at a concentration of 5% after 28 days, reaching 12.25 MPa, with an absorption value of 7.12%. The results of XRF characterization showed that the concentrations of basalt stone and rice husk ash were directly and inversely proportional to the content of CaO and SiO<sub>2</sub>, respectively. Based on XRD characterization, the phases formed were ternesite, microline maximum, and yeelimite.*

**Keywords:** Paving block, ash, rice husk, basalt, characterization.

## I. INTRODUCTION

Paving block (concrete brick) is an alternative for ground surface pavement layers. It is characterized by easy installation, relatively inexpensive maintenance, and appealing appearance. The block (concrete brick) is made up of building materials from a mixture of portland cement or other hydraulic adhesives [1]. The use of paving block supports environmental sustainability initiatives promoted both nationally and internationally, as water absorption through the installation can maintain groundwater balance [2]. The quality depends on the composition of the basecoat and undercoat, which should be formulated appropriately [3]. A good understanding in terms of the quality and selling price of paving block in the community will enhance interest in the usage for roads and yards [4].

Rice husk is a by-product or waste from the rice milling industry. Approximately 65% rice and 20% rice husk are produced in the industry. Currently, rice husk

has been developed as a raw material for producing rice husk ash (RHA) through the process of burning. At 400-500°C and greater than 1000°C, the ash produced becomes amorphous silica and crystalline silica, respectively. Amorphous silica is considered an important source for manufacturing pure silicon, silicon carbide, and silicon nitride flour [5]. The main components of rice husk ash are cellulose (50%), lignin (30%), and organic compounds (20%) [6]. Based on observation, rice husk ash is a major environmental threat that causes damage to the soil and environment around landfills [7].

Basalt is classified as an igneous rock, chemically rich in oxides of magnesium, calcium, sodium, potassium, silicon, and iron. The stone can be used as an alternative raw material for Portland cement [8]. It originates from volcanic magma and flood volcanoes, a very hot liquid or semi-fluid material beneath the Earth's crust, condensing in the open air [9]. Basalt is generally only used as a foundation for roads, bridges,

buildings, or an aggregate. The rock contains a chemical composition of 56.15% SiO<sub>2</sub>, 17.37% Al<sub>2</sub>O<sub>3</sub>, 4.62% Fe<sub>2</sub>O<sub>3</sub>, 8.25% CaO, 6.90% MgO, 3.28% K<sub>2</sub>O, 99% TiO, and MnO of 0.46% [10]. Based on [11], the content, the composition of SiO<sub>2</sub> + Fe<sub>2</sub>O<sub>3</sub> + Al<sub>2</sub>O<sub>3</sub> generates a minimum of 70%.

In this study, paving block is made using basalt stone and rice husk ash with variations of 0%, 5%, 10%, 15%, 20% and 25%. The block is soaked in water for 7, 14, and 28 days before further tests for compressive strength, specific gravity, porosity, and absorption. Characterization by X-Ray Diffraction (XRD) and X-Ray Fluorescence (XRF) was conducted to determine the crystal phase and chemical composition, respectively.

## II. MATERIALS AND METHODS

### A. Tools and Materials

The tools used are a ball mill, mixer, beaker glass, 5×5×5 cm mortar molds, analog scales, digital scales, ovens, measuring cups, mesh sieves, compressive strength testing machines, XRF testing machines, XRD testing machines, buckets, cup, plastic zipper, spatula, agate mortar, and pastel. The materials include basalt stone from East Lampung, cement type PCC, sand from Labuhan Maringgai, East Lampung, water from Tanjung Bintang, and rice husk ash.

### B. Methods

In the first step, basalt stone was prepared by grinding with a ball mill for ± 6 hours, sieving using 5 and 10 mesh passes, before characterization by XRF and XRD. The second step includes preparing RHA by burning rice husk, pounding using a mortar and pestle, and characterization by XRF and XRD.

**Table 1.** Material composition

| No | Material           | Variation (%) |       |      |       |     |        |
|----|--------------------|---------------|-------|------|-------|-----|--------|
|    |                    | 0             | 5     | 10   | 15    | 20  | 25     |
| 1  | Cement (gr)        | 150           | 150   | 150  | 150   | 150 | 150    |
| 2  | Sand (gr)          | 850           | 807,5 | 765  | 722,5 | 680 | 637,5  |
| 3  | Basalt Stone (gr)  | 0             | 21,2  | 42,5 | 63,7  | 85  | 106,25 |
| 4  | Rice Husk Ash (gr) | 0             | 21,2  | 42,5 | 63,7  | 85  | 106,25 |
| 5  | Water (ml)         | 100           | 100   | 100  | 100   | 100 | 100    |

In the next stage, paving block is produced by mixing all ingredients such as cement, sand, basalt stone, rice husk ash, and water. The cement and sand were weighed according to the composition ratio of 1:6, while basalt stone and rice husk ash were measured based on the respective addition concentrations to sand, namely 0%, 5%, 10%, 15%, 20%, and 25%. All these ingredients were mixed into a container by adding 100

ml of water. The mixture was stirred using a mixer for 20 minutes until homogeneous. Furthermore, the same repetition was conducted for each variation in the concentration of adding basalt stone and rice husk ash to the sand. The mixture was printed using a 5 × 5 × 5 cm mortar mold, left for 24 hours at room temperature, before being released as a test object (sample). The samples were further immersed in clean water for 7 days, 14 days, and 28 days. Tests, including compressive strength, specific gravity, porosity, and absorption tests, were conducted. Finally, the samples were characterized based on XRF and XRD.

## III. RESULTS AND DISCUSSIONS

### A. Basalt Testing Results

**Table 2.** Results of XRF characterization of basalt stone

| No | Compound                       | Percentage (%) |
|----|--------------------------------|----------------|
| 1  | SiO <sub>2</sub>               | 43,023         |
| 2  | Fe <sub>2</sub> O <sub>3</sub> | 21,614         |
| 3  | Al <sub>2</sub> O <sub>3</sub> | 14,795         |
| 4  | MgO                            | 2,362          |
| 5  | TiO <sub>2</sub>               | 1,723          |
| 6  | P <sub>2</sub> O <sub>5</sub>  | 0,753          |
| 7  | K <sub>2</sub> O               | 0,704          |
| 8  | MnO                            | 0,64           |
| 9  | Cr <sub>2</sub> O <sub>3</sub> | 0,112          |

XRF characterization results of basalt are shown in **Table 2**. Samples with the highest oxide compound content, namely SiO<sub>2</sub> of 43.023%, Fe<sub>2</sub>O<sub>3</sub> of 21.614%, Al<sub>2</sub>O<sub>3</sub> of 14.795%, MgO of 2.362%, TiO<sub>2</sub> of 1.723%, P<sub>2</sub>O<sub>5</sub> of 0.753%, K<sub>2</sub>O of 0.704%, MnO of 0.641%, and Cr<sub>2</sub>O<sub>3</sub> of 0.112% are presented. Basalt has pozzolanic properties according to ASTM C168, where SiO<sub>2</sub> + Al<sub>2</sub>O<sub>3</sub> + Fe<sub>2</sub>O<sub>3</sub> generate a minimum of 70%. In this study, the value was recorded at 79%, hence can be used as a pozzolanic material that meets ASTM requirements. The results of XRD characterization on basalt rock are presented in **Figure 1**.

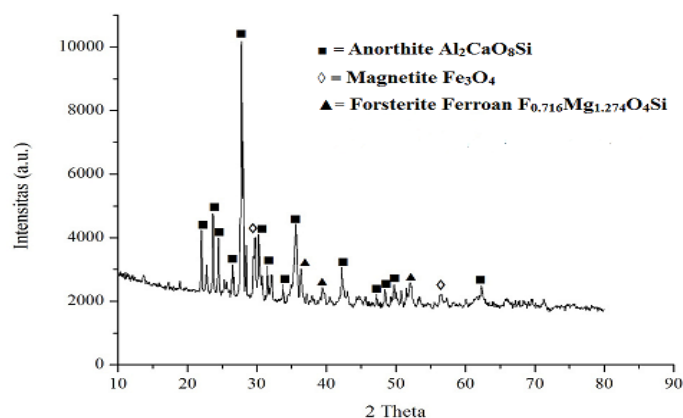


**Figure 1.** XRD spectrum of basalt stone sample.

The diffraction peaks were predominantly associated with *anorthite*, an ordered ( $\text{Al}_2\text{CaO}_3\text{Si}_2$ ) with ref. code ICDD 00-041-1486, featuring the highest intensity at  $2\theta = 27.78^\circ$ . Another major phase identified is *magnetite* ( $\text{Fe}_3\text{O}_4$ ) with ref. code ICDD 01-089-0951, presenting a prominent peak at  $2\theta = 29.738^\circ$ . In addition, a ferroan forsterite (Ca-doped) ( $\text{Fe}_{0.716}\text{Mg}_{1.274}\text{O}_4\text{Si}$ ) phase was detected, corresponding to ref. ICDD code 01-071-0794, with its highest peak at  $2\theta = 36.325^\circ$ . The results suggest that the basalt sample contains major minerals such as *anorthite*, *ordered* or *calcium aluminum silicate* ( $\text{Al}_2\text{CaO}_3\text{Si}_2$ ), *magnetite* or *iron oxide* ( $\text{Fe}_3\text{O}_4$ ), and *ferroan forsterite* or *magnesium iron silicate* ( $\text{Fe}_{0.716}\text{Mg}_{1.274}\text{O}_4\text{Si}$ ).

### B. Rice Husk Ash Testing Results

**Table 3.** Results of XRF characterization of rice husk ash

| No | Compound                | Percentage (%) |
|----|-------------------------|----------------|
| 1  | $\text{SiO}_2$          | 84,557         |
| 2  | $\text{K}_2\text{O}$    | 7,465          |
| 3  | $\text{CaO}$            | 3,530          |
| 4  | $\text{P}_2\text{O}_5$  | 2,134          |
| 5  | $\text{SO}_3$           | 1,075          |
| 6  | $\text{Fe}_2\text{O}_3$ | 0,437          |
| 7  | $\text{MgO}$            | 0,367          |
| 8  | $\text{MnO}$            | 0,306          |

XRF characterization of rice husk ash is shown in **Table 3**. Ash sample features the highest oxide compound content, respectively, including  $\text{SiO}_2$  of 84.557%,  $\text{K}_2\text{O}$  of 7.465%,  $\text{CaO}$  of 3.530%,  $\text{P}_2\text{O}_5$  of 2.134 %,  $\text{SO}_3$  of 1.075%,  $\text{Fe}_2\text{O}_3$  of 0.437%,  $\text{MgO}$  of 0.367% and  $\text{MnO}$  of 0.306%. The highest was  $\text{SiO}_2$  used as filler material in making paving block, corresponding with the study by [12]. The results of XRD characterization on rice husk ash are presented in **Figure 2**.

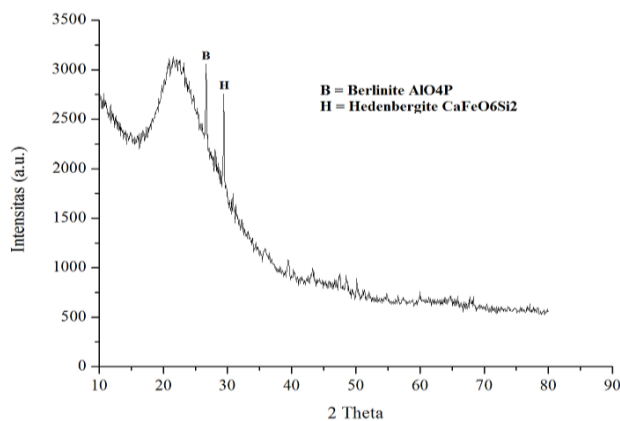


**Figure 2.** XRD spectrum of rice husk ash sample

The results of XRD characterization of rice husk ash

are shown in **Figure 2**. The diffraction pattern is dominated by a peak corresponding to *hedenbergite*, *syn* ( $\text{CaFeO}_6\text{Si}_2$ ), with ref code ICDD 01-071-1502, featuring the most intense peak at  $2\theta = 29.387^\circ$ . Another prominent phase identified was *berlinite*, *syn* ( $\text{AlO}_4\text{P}$ ) with ref code ICDD 01-076-0228, showing its highest peak at  $2\theta = 26.666^\circ$ .

### C. Sand Testing Result

**Table 4.** Results of sand XRF characterization

| No | Compound                | Percentage (%) |
|----|-------------------------|----------------|
| 1  | $\text{SiO}_2$          | 61,846         |
| 2  | $\text{Al}_2\text{O}_3$ | 18,636         |
| 3  | $\text{Fe}_2\text{O}_3$ | 10,182         |
| 4  | $\text{K}_2\text{O}$    | 4,237          |
| 5  | $\text{TiO}_2$          | 2,036          |
| 6  | $\text{CaO}$            | 1,631          |
| 7  | $\text{P}_2\text{O}_5$  | 0,788          |
| 8  | $\text{ZrO}_2$          | 0,259          |

XRF characterization results of sand are shown in Table 4. The predominant oxide compounds were  $\text{SiO}_2$  of 61.846%,  $\text{Al}_2\text{O}_3$  of 18.636%,  $\text{Fe}_2\text{O}_3$  of 10.182%,  $\text{K}_2\text{O}$  of 4.237%,  $\text{TiO}_2$  of 2,036%,  $\text{CaO}$  of 1,631%,  $\text{P}_2\text{O}_5$  of 0,788%, and  $\text{ZrO}_2$  of 0,259%. The relatively high  $\text{Al}_2\text{O}_3$  content suggested the presence of mud in a significant amount. Silica content in the sand functioned as a filler material, while the lime content played a role in the binding process [13].

The results of XRD characterization on sand can be seen in **Figure 3**.

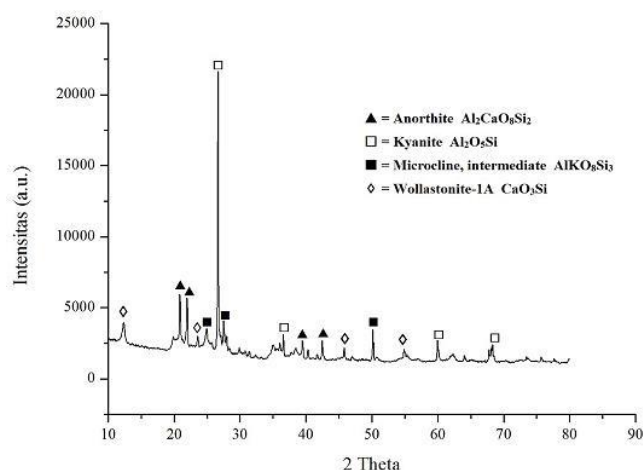


**Figure 3.** XRD spectrum of the sand sample.

The diffraction pattern is dominated by a peak corresponding to *kyanite* ( $\text{Al}_2\text{O}_5\text{Si}$ ), with ref code ICDD 01-074-1827, featuring the highest intensity at  $2\theta = 26.627^\circ$ . Another phase identified was *anorthite* phase ( $\text{Al}_2\text{CaO}_8\text{Si}_2$ ), with ref. ICDD code 01-089-1460, presenting a prominent peak at  $2\theta = 20.939^\circ$ . *Microcline, intermediate* ( $\text{AlKO}_8\text{Si}_3$ ) was also

detected, with ref. ICDD code 00-019-0932 and the highest peak at  $2\theta = 50.167^\circ$ . Additionally, wollastonite-1A (CaO3Si) was detected, with ref. ICDD code 01-073-1110, featuring the highest peak at  $2\theta = 12,427^\circ$ .

#### D. Paving Block Physical Test Results

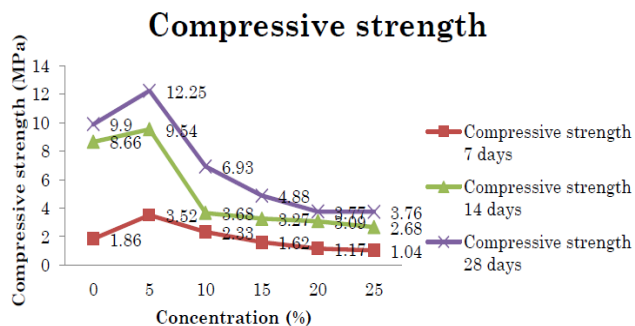


**Figure 4.** Graph of paving block compressive strength test results

The results of the paving block compressive strength test are shown in **Figure 4**. The weight concentration of basalt stone and rice husk ash affected the compressive strength of the paving block. Based on observation, the maximum concentration was recorded to be 5%. The greater the compressive strength value, the better the quality and quality of paving block [14]. The high compressive strength is due to the bonding of cement and aggregates. This strength was further influenced by the pozzolanic reaction of additional materials derived from basalt rock and rice husk ash [15].

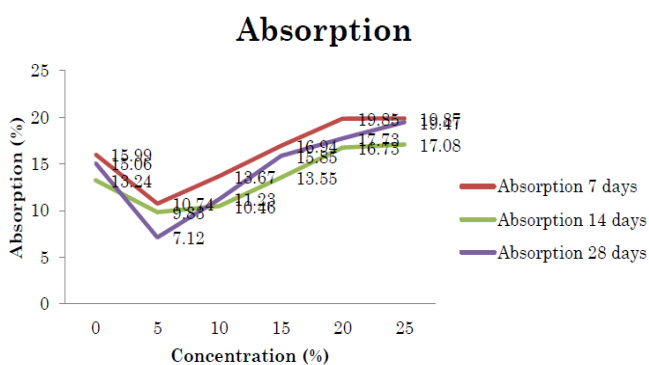


**Figure 5.** Graph of paving block absorption test results

The results of paving block absorption test are shown in **Figure 5**. The weight concentration of basalt stone and rice husk ash affected the absorption value of the paving block [16]. Based on observation, the concentration at 5% had the lowest decrease in absorption value, which is inversely proportional to the

compressive strength. The lower the absorption value (water absorption) of the paving block, the better the quality. The magnitude of absorption depends on the density and number of cavities contained in the block [17].

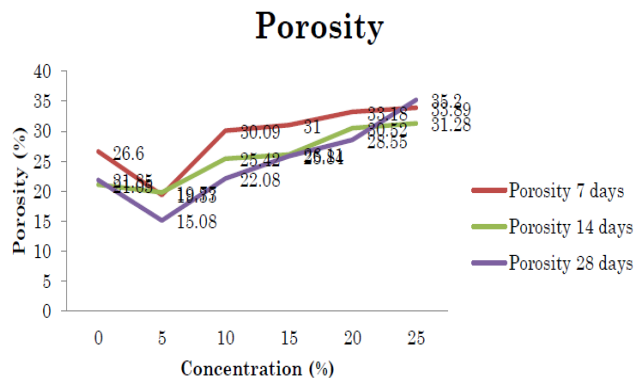


**Figure 6.** Graph of paving block porosity test results

The results of paving block porosity test are shown in **Figure 6**. The weight concentration of basalt stone and rice husk ash affected the value of paving block porosity. Based on observation, the concentration at 5% featured the smallest reduction in porosity, while at 10%, 15%, 20%, and 25%, progressively increased porosity was recorded. This is because, alongside the rise in the percentage of basalt stone and rice husk ash, the high increase in paving block was influenced by the making process [18].

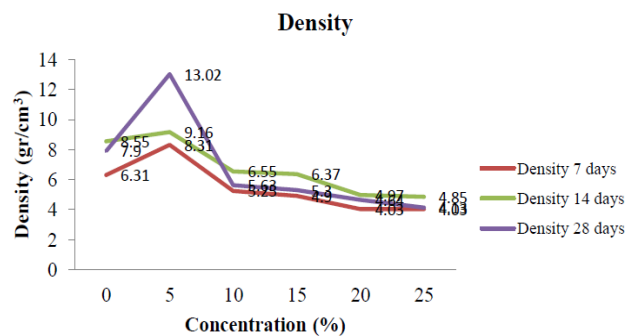


**Figure 7.** Graph of density test results for paving block

The results of paving block density test are shown in **Figure 7**. The concentration of basalt stone weight and rice husk ash affected the density value of the paving block. Based on observation, the maximum value was observed at 5%. The addition of higher concentrations tends to reduce the density of paving block [19]. The density is directly proportional to the compressive strength and the quality of the block.

## E. Paving Block Characterization Results

**Table 5.** Results of XRF characterization of paving block

| No | Compound                       | Percentage 0% | Percentage 5% | Percentage 25% |
|----|--------------------------------|---------------|---------------|----------------|
| 1  | CaO                            | 43,013        | 41,296        | 43,118         |
| 2  | SiO <sub>2</sub>               | 33,123        | 35,304        | 36,708         |
| 3  | Al <sub>2</sub> O <sub>3</sub> | 9,404         | 9,081         | 7,147          |
| 4  | Fe <sub>2</sub> O <sub>3</sub> | 9,223         | 8,955         | 8,172          |
| 5  | K <sub>2</sub> O               | 2,481         | 2,780         | 2,407          |
| 6  | TiO <sub>2</sub>               | 1,381         | 1,360         | 1,087          |
| 7  | SO <sub>3</sub>                | 0,585         | 0,610         | 0,546          |
| 8  | MgO                            | 0,174         | -             | 0,213          |
| 9  | SrO                            | 0,174         | 0,166         | 0,177          |
| 10 | MnO                            | 0,129         | 0,138         | 0,170          |

The results of XRF characterization of paving block are shown in **Table 5**. Furthermore, the predominant oxide compounds include CaO, SiO<sub>2</sub>, Fe<sub>2</sub>O<sub>3</sub>, and Al<sub>2</sub>O<sub>3</sub> in decreasing order. The decrease in CaO content at the 5% concentration was attributed to the composition of rice husk ash, which contains a high proportion of SiO<sub>2</sub> and a low proportion of CaO. Meanwhile, cement had a high CaO content and relatively low SiO<sub>2</sub> content. The increase in SiO<sub>2</sub> at concentrations of 0%, 5% and 25% was due to its high content in rice husk ash and basalt stone.

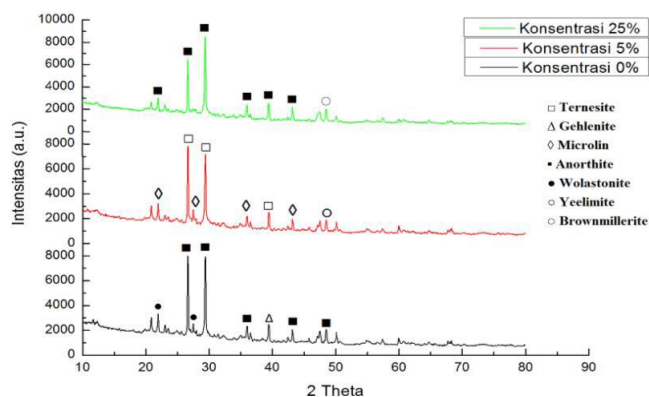


**Figure 8.** XRD spectrum of a paving block sample

The results of XRD characterization of paving block are shown in **Figure 8**. At a concentration of 0%, the formed phase is *anorthite* (Ca(Al<sub>2</sub>Si<sub>2</sub>O<sub>8</sub>)), *wollastonite-1A* (CaSiO<sub>3</sub>), and *gehlenite* (Ca<sub>2</sub>(AlSi)O<sub>7</sub>). The highest phase was *anorthite* (Ca(Al<sub>2</sub>Si<sub>2</sub>O<sub>8</sub>)) with the highest peak intensity located at 2θ = 29.337°. At a concentration of 5%, the formed phases were *ternesite* (Ca<sub>5</sub>(SiO<sub>4</sub>)<sub>2</sub>SO<sub>4</sub>), *microcline* (KAlSi<sub>3</sub>O<sub>8</sub>), and *yeelimite* (Ca<sub>4</sub>Al<sub>6</sub>O<sub>12</sub>SO<sub>4</sub>). The highest was *ternesite* (Ca<sub>5</sub>(SiO<sub>4</sub>)<sub>2</sub>SO<sub>4</sub>), with the highest peak intensity located at 2θ = 27.886°. At a concentration of 25%, the phases formed were *anorthite* (Ca(Al<sub>2</sub>Si<sub>2</sub>O<sub>8</sub>)) and *brownmillerite* (Ca<sub>2</sub>(Al,Fe+3)O<sub>5</sub>). The highest phase

was *anorthite* (Ca(Al<sub>2</sub>Si<sub>2</sub>O<sub>8</sub>)), with the highest intensity peak located at 2θ = 29.348°. The formation of the *anorthite* (Ca(Al<sub>2</sub>Si<sub>2</sub>O<sub>8</sub>)) phase at concentrations of 0% and 5% can be attributed to the composition of the constituent materials. Cement contributes a high CaO content of 63.22%, basalt provides a substantial amount of Al<sub>2</sub>O<sub>3</sub> at 14.795%, and rice husk ash supplies a high SiO<sub>2</sub> content of 84.557%.

## IV. CONCLUSIONS

In conclusion, basalt stone and rice husk ash were used as additional materials for making paving block. The maximum addition was at a concentration of 5%, which produced a compressive strength value of 12.25 MPa. Paving block was classified into D quality, confirming the usage for parks and others with an average compressive strength of 8.43 MPa.

## ACKNOWLEDGMENT

The authors are grateful to the Head of Mineral Technology Research Institute - LIPI Lampung, the Head of Non-Metal Laboratory, and the Head of Chemical Analysis Laboratory of Mineral Technology Research Institute - LIPI Lampung.

## REFERENCES

- [1] Standar Nasional Indonesia (SNI) 03-0691-1996. *Bata Beton (Paving Block)*. Badan Standardisasi Nasional.
- [2] Adibroto, F. 2014. Pengaruh Penambahan Berbagai Jenis Serat pada Kuat Tekan *Paving Block*. *Jurnal Rekayasa Sipil*. Vol. 10. No. 1. Pp. 1-11.
- [3] Charin, N., Chaiwut, B., Weerachat, T., dan Chai, J. 2018. Development of Concrete Paving Blocks Prepared from Waste Materials without Portland Cement. *Materials Science*. Vol. 24. No. 1. ISSN 1392-1320.
- [4] Syukur, S., Wayan, D., dan Alexander, P. 2011. Perbandingan Mutu *Paving Block* Produksi Manual Dengan Produksi Masinal. *Jurnal Rekayasa*. Vol. 15. No. 2.
- [5] Desniati, Emmi. 2013. *Studi Kekuatan Paving Block Pasca Pembakaran Menggunakan Material Tanah Lempung dan Semen serta Abu Sekam Padi untuk jalan lingkungan*. Bandar Lampung: Universitas Lampung.
- [6] Fernandes, I.J., Calheiro, D., Kieling, A.G., Moraes, C.A.M., Rocha, T.L.A.C., Brehm, F.A., and

- Modolo, R.C.E. 2016. Characterization of rice husk ash produced using different biomass combustion techniques for energy. *Fuel*. 165. 351–359.
- [7] Ankit, G., Rahul, B., dan Nishant, S. 2019. A Study On Use Of Rice Husk Ash In Concrete. *Engineering Heritage Journal (GWK)*. Vol. 3. No. 1. Pp. 01-04.
- [8] Vishal, P, K. 2014. Basalt Rock Fibres New Construction Material. *Acta Engineering International*. Vol. 2. No. 1. Pp 11-18.
- [9] Karyanto. 2004. Cross Diagonal Survey Geolistrik Tahanan Jenis 3D untuk Menentukan Pola Penyebaran Batuan Basal di Daerah Pakuan Aji Lampung Timur. *Jurnal Sains Teknologi*. Vol. 10. No. 3. Pp 195-200.
- [10] Amin, M., dan Suharto. 2017. Pembuatan Semen Geopolimer Ramah Lingkungan Berbahan Baku Mineral Basal Guna Menuju Lampung Sejahtera. *Jurnal Kelitbangan*. Vol. 5. No. 1.
- [11] ASTM C168. 2003. Standard Specification for Coal Fly Ash and Raw or Calcined Natural Pozzolan for Use in Concrete. Annual Books of ASTM standards. USA.
- [12] Bakri. 2008. Komponen Kimia dan Fisik Abu Sekam Padi Sebagai SCM untuk Pembuatan Komposit Semen. *Jurnal Perennial*. Vol. 5. No. 1. Pp. 9-14.
- [13] Alfian, U., Ir. Utari, K, MT., dan Ir. Soerjandani, PM, MT. 2018. Pasir Kuarsa Tuban Sebagai Bahan Substitusi Semen Dan Batu Pecah Substitusi Pasir Untuk Campuran Paving. *Jurnal Rekayasa dan Manajemen Kontruksi*. Vol. 6. No. 1. Pp. 47-52.
- [14] Agustina, D, S., Zakki, R, M., Achmad, C, S., dan Erika, R. 2017. Pembuatan Batako dengan Campuran *Fly Ash* dan Styrofoam. *Jurnal Ilmiah Teknik Kimia*. Vol. 1. No. 1. Pp 1-7.
- [15] Didik, H., Endang, K., Boedi, W., dan Sulchan, A. 2014. Penambahan Abu Ampas Tebu (AAT) dan Limbah Boma Bisma Indra (BBI) untuk Pembuatan *Paving Block*. *Jurnal Aplikasi*. Vol. 12. No. 1. Pp 17-26
- [16] Diah, L., Iswan., dan Setynto. 2016. Uji Kuat Tekan *Paving Block* Menggunakan Campuran Tanah dan Kapur dengan Alat Pematik Modifikasi. *JRSDD*. Vol. 4. No. 1. Pp. 11-22.
- [17] Artiyani, A. 2010. Pemanfaatan Abu Pembakaran Sampah Sebagai Bahan Alternatif Pembuatan *Paving Block*. *Spectra*. Vol. 8. No. 16. Pp 1-11.
- [18] Kanti, E, P. 2014. Pengaruh Penambahan Limbah Pembakaran Ampas Tebu Pada *Paving Block* Terhadap Jenis Semen PPC dan PCC. *Jurnal Teknik Sipil dan Perencanaan*. Vol. 16. No. 2. Pp 125-134.
- [19] Euniza, J., Hasanah, N., Zaitun, H., Norhidayah, A, H., and Ramadhansyah, J. 2019. Porosity and Density Characteristic of Double-layer Concrete *Paving Blocks* Incorporating Rubber Granules. National Colloquium on Wind and Earthquake Engineering. Vol. 244.